Nanosponge-encapsulated camptothecin exerts anti-tumor activity in human prostate cancer cells

Elsevier Editorial System(tm) for European Journal of Pharmaceutical Sciences
Manuscript Draft

Manuscript Number: EJPS-D-12-00214

Title: NANOSPONGE-ENCAPSULATED CAMPTOTHECIN EXERTS ANTI-TUMOR ACTIVITY IN HUMAN PROSTATE CANCER CELLS.

Article Type: Full Length Article

Keywords: Prostate Cancer, Camptothecin, β-cyclodextrin nanosponge, DNA Topoisomerase I, DNA damage, Androgen Receptor.

Corresponding Author: Ph.D. Chiara Dianzani, Ph.D.

Corresponding Author's Institution: Department of Drug Science and Technology - University of Turin, Via P. Giuria 9, 10125 Turin Italy.

First Author: Rosalba Minelli, Ph.D.

Order of Authors: Rosalba Minelli, Ph.D.; Roberta Cavalli, Professor; Leigh Ellis, Ph.D.; Piergiorgio Pettazzoni, Ph.D.; Francesco Trotta, Professor; Eric Ciamporcero; Giuseppina Barrera, Professor; Roberto Fantozzi, Full professor; Chiara Dianzani, Ph.D.; Roberto Pili, M.D,

Manuscript Region of Origin: ITALY

Abstract: Camptothecin (CPT) is a potent DNA Topoisomerase I inhibitor with anti-tumor activity in haematological and solid tumors. However, it did not reach clinical use because of its poor solubility and high degrability. In the present study, we evaluated whether β-cyclodextrin nanosponge carriers can overcome CPT chemical disadvantages and improve the in vitro anti-tumor efficacy in the androgen refractory models of prostate cancer DU145 and PC-3 and the androgen sensitive model LNCaP. HPLC analysis, performed on the cell pellet after treatment with CPT-loaded β-cyclodextrin nanosponge (CN-CPT) revealed that CPT concentration increased over time indicating a prolonged release of the drug. Moreover, CN-CPT inhibited Topoisomerase I activity, DNA damage, and cell cycle arrest indicating that the CN-CPT formulation does not affect activity of the drug. CN-CPT exerted an increased anti-tumor activity, in both models, as compared to CPT. Moreover, Annexin V/Propidium Iodide staining showed an induction of cell death at low concentrations that were not effective for CPT. LNCaP cells were less sensitive to CPT than PC-3 and DU145 cells, but CN-CPT still exerted higher anti-proliferative activity and DNA damage ability than CPT. Moreover in LNCaP cells, CN-CPT treatment inhibited expression of the androgen receptor at doses where CPT was ineffective. Taken together these results support the use of the β-cyclodextrin nanosponge technology to deliver anticancer drugs for the treatment of both androgen sensitive and castrate-refractory prostate cancers.

Abstract

Camptothecin (CPT) is a potent DNA Topoisomerase I inhibitor with anti-tumor activity in haematological and solid tumors. However, it did not reach clinical use because of its poor solubility and high degrability. In the present study, we evaluated whether β-cyclodextrin nanosponge carriers can overcome CPT chemical disadvantages and improve the *in vitro* anti-tumor efficacy in the androgen refractory models of prostate cancer DU145 and PC-3 and the androgen sensitive model LNCaP. HPLC analysis, performed on the cell pellet after treatment with CPT-loaded β-cyclodextrin nanosponge (CN-CPT) revealed that CPT concentration increased over time indicating a prolonged release of the drug. Moreover, CN-CPT inhibited Topoisomerase I activity, DNA damage, and cell cycle arrest indicating that the CN-CPT formulation does not affect activity of the drug. CN-CPT exerted an increased anti-tumor activity, in both models, as compared to CPT. Moreover, Annexin V/Propidium Iodide staining showed an induction of cell death at low concentrations that were not effective for CPT. LNCaP cells were less sensitive to CPT than PC-3 and DU145 cells, but CN-CPT still exerted higher anti-proliferative activity and DNA damage ability than CPT. Moreover in LNCaP cells, CN-CPT treatment inhibited expression of the androgen receptor at doses where CPT was ineffective. Taken together these results support the use of the β-cyclodextrin nanosponge technology to deliver anticancer drugs for the treatment of both androgen sensitive and castrate-refractory prostate cancers.

Keywords: Prostate Cancer, Camptothecin, β-cyclodextrin nanosponge, DNA Topoisomerase I, DNA damage, Androgen Receptor.

Graphical Abstract (for review)

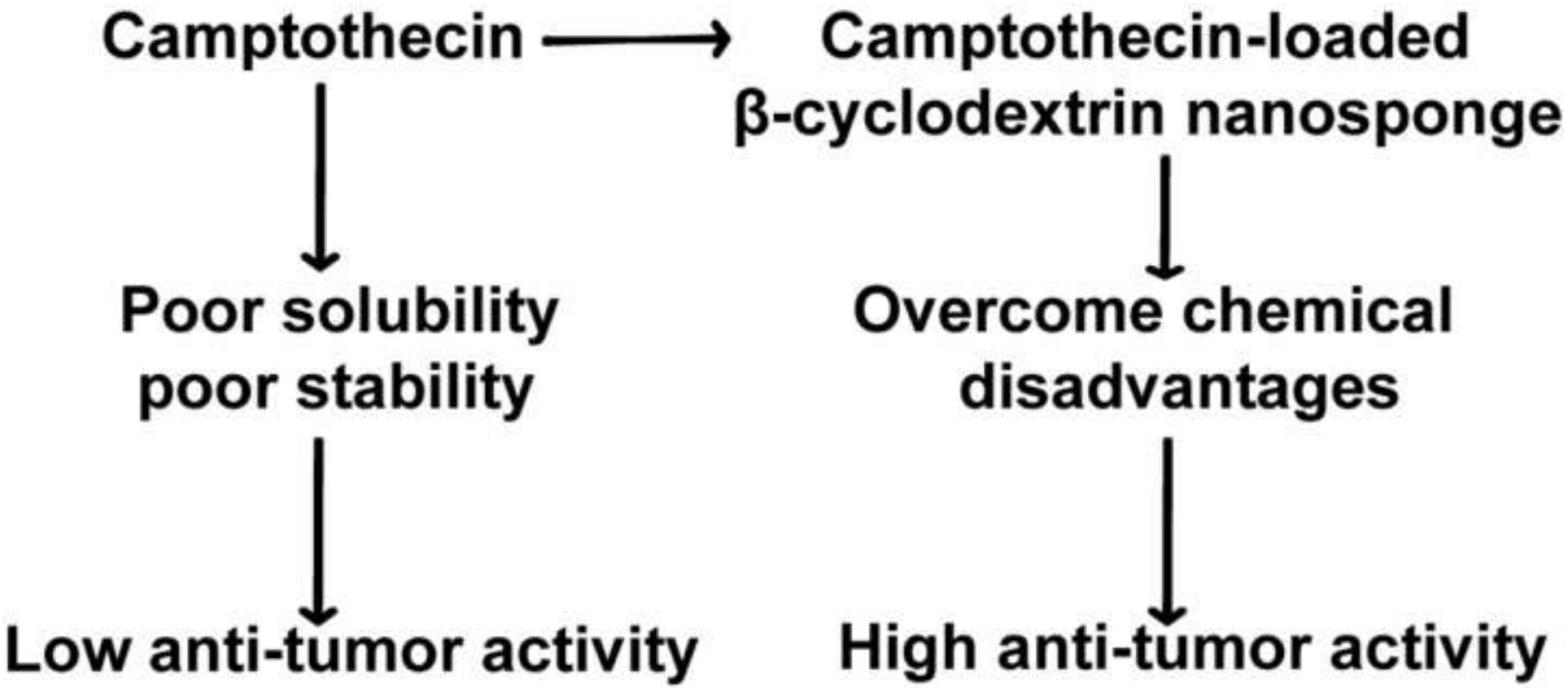

NANOSPONGE-ENCAPSULATED CAMPTOTHECIN EXERTS ANTI-TUMOR ACTIVITY IN HUMAN PROSTATE CANCER CELLS.

Rosalba Minelli[a,b], Roberta Cavalli[a], Leigh Ellis[b], Piergiorgio Pettazzoni[b,c], Francesco Trotta[d], Eric Stefano Ciamporcero[c], Giuseppina Barrera[c], Roberto Fantozzi[a], Chiara Dianzani[a]* and Roberto Pili[b]*.

[a] Department of Drug Science and Technology - University of Turin, Via P. Giuria 9, 10125 Turin Italy.

[b] Genitourinary Program-Roswell Park Cancer Institute, Elm & Carlton Streets 14263 Buffalo-NY USA.

[c] Medicine and Experimental Oncology - Section of General Pathology- University of Turin, Corso Raffaello 30, 10125 Turin Italy.

[d] Department of Chemistry I.F.M - University of Turin, Via P. Giuria 7, 10125 Turin Italy.

***Corresponding authors:**
Chiara Dianzani PhD
Department of Drug Science and Tecnology
University of Turin
Via P. Giuria 9
10125 Torino – ITALY
chiara.dianzani@unito.it
Tel:0039-011-670-7690
Fax:0039-011-670-7688

Roberto Pili MD
Genitourinary Program
Roswell Park Cancer Institute
Elm & Carlton Streets
Buffalo NY 14263
Roberto.Pili@Roswellpark.org
Tel:001-716-845-3851
Fax:001-716-845-8232

Abstract

Camptothecin (CPT) is a potent DNA Topoisomerase I inhibitor with anti-tumor activity in haematological and solid tumors. However, it did not reach clinical use because of its poor solubility and high degrability. In the present study, we evaluated whether β-cyclodextrin nanosponge carriers can overcome CPT chemical disadvantages and improve the *in vitro* anti-tumor efficacy in the androgen refractory models of prostate cancer DU145 and PC-3 and the androgen sensitive model LNCaP. HPLC analysis, performed on the cell pellet after treatment with CPT-loaded β-cyclodextrin nanosponge (CN-CPT) revealed that CPT concentration increased over time indicating a prolonged release of the drug. Moreover, CN-CPT inhibited Topoisomerase I activity, DNA damage, and cell cycle arrest indicating that the CN-CPT formulation does not affect activity of the drug. CN-CPT exerted an increased anti-tumor activity, in both models, as compared to CPT. Moreover, Annexin V/Propidium Iodide staining showed an induction of cell death at low concentrations that were not effective for CPT. LNCaP cells were less sensitive to CPT than PC-3 and DU145 cells, but CN-CPT still exerted higher anti-proliferative activity and DNA damage ability than CPT. Moreover in LNCaP cells, CN-CPT treatment inhibited expression of the androgen receptor at doses where CPT was ineffective. Taken together these results support the use of the β-cyclodextrin nanosponge technology to deliver anticancer drugs for the treatment of both androgen sensitive and castrate-refractory prostate cancers.

Keywords: Prostate Cancer, Camptothecin, β-cyclodextrin nanosponge, DNA Topoisomerase I, DNA damage, Androgen Receptor.

1. Introduction

Prostate cancer (PCa) is the most frequently diagnosed non-cutaneous malignancies and is the second cause of death among cancers in Americans and Western European males (Droz and Chaladaj, 2008; Shen and Abate-Shen, 2010). Though recurrent PCa presents, initially, androgen-sensitive growth, eventually it escapes from the hormonal control and develops into castrate-refractory disease (Feldman and Feldman, 2001; Taplin, 2007), where chemotherapeutic agents such as microtubule inhibitors have shown clinical benefit but of limited duration.

While novel drugs are currently under investigation for the treatment of both androgen-sensitive and castrate-refractory PCa, recent advances in drug delivery technology allowed to re-evaluate available drugs that had been previously discarded because of the unsatisfactory efficacy or unacceptable toxicity. Indeed, such technologies may lead to more efficient intra-tumor drug delivery, improved availability and pharmacological properties resulting in increased therapeutic index (Bharali et al., 2009; Zhang et al., 2008).

β-cyclodextrin nanosponge are solid nanoparticles developed to deliver both hydrophilic and hydrophobic compounds (Trotta and Cavalli, 2009). Their structure consists of a hyper-cross-linked cyclodextrin matrix that constitutes a protected environment capable to transport different molecules, even with a relatively complex structure (Cavalli et al., 2006; Swaminathan et al., 2007). The advantage of this technology consists, primarily, in solubility capacities and in the protection of easily degradable compounds from the external environment, allowing the delivery of insoluble compounds. Moreover, β-cyclodextrin nanosponge may mediate the controlled release of encapsulated compounds

over time leading to a prolonged exposure, which in turn may reduce the dosage and the frequency of drug administrations. In addition, the β-cyclodextrin polymer per se showed limited toxicity and a good pharmacokinetic profile resulting in a promising emerging tool in drug delivery research (Swaminathan et al., 2010).

Camptothecin (CPT) is a pentacyclic alkaloid isolated from the Chinese tree Camptotheca acuminata showing a significant DNA Topoisomerase I inhibition activity (Wall et al., 1966; Hertzberg et al., 1989). Since DNA Topoisomerases are involved in DNA control by unwinding during DNA replication, the inhibition of these enzymes results in the accumulation of DNA breaks (Pommier, 2006). Following DNA Topoisomerase inhibition, cells undergo either cell cycle arrest in S-phase or progression with subsequent accumulation of DNA damage resulting in cell death (Jones et al., 2000; Takahashi et al., 2011; Zhou et al., 2002). The anti-tumor activity of CPT has been extensively investigated in both hematological and solid malignancies, but its use remained limited due to its poor solubility and high instability. In particular, the CPT molecule presents a lactone ring highly susceptible to hydrolysis in physiological conditions that compromises its Topoisomerase I binding activity (Venditto and Simanek, 2010). Finally, CPT exerts toxicity in normal tissues including myelosuppression and hemorrhagic cystitis (Koo et al., 2005).

To overcome these pharmacological disadvantages, we have tested the possibility of using β-cyclodextrin nanosponge technology to improve CPT delivery to tumor cells and its anti-tumor efficacy in prostate cancer, using both androgen-refractory (DU145 and PC-3) and sensitive (LNCaP) cell lines.

2. Materials and methods

2.1 Compounds

Camptothecin (CPT) was purchased from Sigma-Aldrich and dissolved in dimethyl sulfoxide (DMSO). β-cyclodextrin nanosponge were prepared as described elsewhere (Swaminathan et al., 2010).

2.2 Characterization of nanosponge-encapsulated Camptothecin

The nanosponge formulation was prepared as previously reported (Swaminathan et al., 2010).

The average diameters and polydispersity indices of CN-CPT were determined by photocorrelation spectroscopy (PCS) using a 90 Plus instrument (Brookhaven, NY, USA) at a fixed angle of 90° and a temperature of 25°C. The water nanosuspension was diluted 1:30 v/v before analysis. Each reported value is the average of ten measurements. The polydispersity index is the size distribution of the nanoparticle population. The electrophoretic mobility and zeta potential of CN-CPT were determined using a 90 Plus instrument (Brookhaven, NY, USA). For zeta potential determination, the nanosuspension was diluted with KCl 0.1 mM and placed in the electrophoretic cell, where an electric field of about 15 V/cm was applied. The sample was analyzed at least in triplicate.

Transmission electron microscopy (TEM) analysis was performed using a Philips CM10 (Eindoven, NL) instrument. For this purpose a CN-CPT aqueous suspension was sprayed on a copper grid.

2.3 Primary antibodies

Anti-p-H2A.X (ser 139) (05-636) antibody was purchased from Millipore, anti-AR (sc-816) from Santa Cruz Biotechnology, and anti β-actin (A1978) from Sigma-Aldrich.

2.4 Cell and culture conditions

DU145, PC-3, and LNCaP cells were obtained from the American Type Culture Collection and were cultured in RPMI 1640 (Gibco) supplemented with 5% penicillin-streptomycin (Gibco) and 10% fetal calf serum (Gibco) in a humidified atmosphere with 5% CO_2.

2.5 Cell proliferation

MTT (3-(4,5-Dimethylthiazol-2-yl)-2,5diphenyltetrazolium bromide) analysis was performed in 96-well plates. Briefly, 800-1500 cells/well were seeded in 200 µl of complete medium and treated with the compounds after 24 hours. Subsequently, cells were supplemented with 25 µl of 5 mg/ml thiazolyl blue tetrazolium bromide (M2128; Sigma-Aldrich) for 2 hours. Thereafter, the medium was removed and cells were lysed with 100 µl of DMSO. Absorbance was recorded at 570 nm by a 96-well-plate ELISA reader.

2.6 Colony-forming assay

Cells (500/well) were seeded into a 6-well plate and treated with the compounds. The medium was changed after 72 hours and cells were cultured for additional 10 days. Subsequently, cells were fixed and stained with a solution of 90% crystal violet (Sigma-Aldrich) and 10% methanol. Colonies were then photographed and counted with a Gel Doc equipment (Bio-Rad Laboratories).

2.7 Determination of CPT cell loading

Camptothecin internalization was evaluated in cell pellets. To extract camptothecin, 500 µl of MeOH were added to cell pellets and mixed by vortex. After sonication for 15 minutes and centrifugation for 5 minutes at 15000 rpm, the supernatant were analyzed by HPLC. Briefly, a Shimadzu instrument model no. LC-9A, equipped with C R5A chromatopac integrator and RF-551 spectrofluorometric detector in isocratic conditions was used. The separation was carried out using an octadecylsilane column with a 5 µm pore size with a mobile phase containing acetonitrile and triethanolamine aqueous solution (1% w/v) in a ratio of 32:68 (v:v) using a fluorescent detector at a λ_{ex} = 360 nm and λ_{em} = 440 nm. The flow rate was kept at 1.0 ml/min. The peak of camptothecin was obtained at a retention time of about 6 min.

2.8 Topoisomerase I extraction and activity

Topoisomerase I activity was evaluated by a commercial kit (1015-1; TopoGEN,Inc.). The extraction was performed according to the manufacturer's instructions.

2.9 Flow cytometry/cell cycle analysis

Adherent and nonadherent cells were collected, washed in 1 XPBS and fixed in 75% ice-cold ethanol and subsequently resuspended in a buffer containing 0.02 mg/ml RNase A (Worthington), 0.05 mg/ml propidium iodide (Sigma-Aldrich), 0.2% v/v Nonidet P-40 (Sigma-Aldrich), 0.1% w/v sodium citrate (Sigma-Aldrich). Samples were analyzed by FACScan flow cytometer (Becton Dickinson).

2.10 Cell death

Adherent and non-adherent cells were collected, washed in 1 XPBS and resuspended in an incubation buffer composed of annexin V binding buffer (556454; BD Pharmingen),

APC-conjugated Annexin V (550474 BD Pharmingen) and 1 μg/ml Propidium Iodide. Cells were analyzed with a FACSCalibur cytometer (Becton Dickinson).

2.11 Immunofluorescence microscopy

Cells were grown on sterile coverslips and treated with the compounds as indicated. Then, cells were fixed with 4% paraformaldehyde for 30 minutes at room temperature, permeabilized by incubation with 0.1% Triton X-100 (Sigma-Aldrich) in 1 XPBS, and blocked with 1% BSA (Sigma-Aldrich) for 1 hour. Cells were further incubated overnight with the primary antibody, washed three times with 1 XPBS, and incubated with Cy3-conjugated donkey anti-mouse antibody (AP192C Millipore). 4´,6-diamidino-2-phenylindole (DAPI) was used to label cell nuclei. Cells were then analyzed by an epifluorescence microscope.

2.12 Lysate preparation and Western blot analysis

Cells were seeded in six well plates and treated as indicated. Lysates were prepared by incubation of cell pellets in a buffer containing 20 mM Tris-HCl, pH 7.4, 150 mM NaCl, 5 mM EDTA, 1% v/v Triton X-100, phosphatase (P2850, Sigma-Aldrich) and protease (P8340) inhibitor cocktails) for 30 minutes at 4°C. The samples were centrifuged at 14,000 rpm for 30 minutes and the supernatants were collected. The protein concentration was determined by a commercially available kit (Bio-Rad Laboratories). 40 μg of protein was mixed with 20 μl of Laemmli sample buffer (161-0737, Bio-Rad Laboratories) containing 10% 2-mercaptoethanol and thereafter boiled for 5 minutes, loaded into the gel (9.3% SDS-polyacrilamyde) and run at constant voltage of 100 V. Subsequently, proteins were transferred onto a nitrocellulose membrane with a semidry transfer apparatus (Biometra) and after blocked with 5% nonfat dry milk, and dissolved in TBS-Tween 20 for 1 hour at

room temperature. After overnight primary antibody incubation at 4°C, the membrane was washed three times with TBS-Tween 20 and further incubated for 1 hour at room temperature with HRP-conjugated secondary antibody (Bio-Rad Laboratories). The detection of bands was carried out through film autoradiography (sc-201697, Santa Cruz Biotechnology).

2.13 Statistical analysis

Data are shown as mean ± SD. One-way ANOVA and the Dunnett's test were used for statistical analysis using Prism 3.0 software (GraphPad Software, La Jolla, CA). Values of $p<0.05$ were considered statistically significant.

3. Results

3.1 Characterization and efficacy of nanosponge-encapsulated Camptothecin

Camptothecin loading nanosponge (CN-CPT) was approximately 38% w/w. The surface charge was negative with a zeta potential value of -25 mV. The average diameter of CN-CPT was about 400 nm with a narrow size distribution. CN-CPT was a stable aqueous nanosuspension with low polydispersity index (Fig. 1A). TEM analysis showed a spherical morphology and confirmed the small size (Fig. 1B). Efficacy of β-cyclodextrin nanosponges to deliver camptothecin in cancer cells was evaluated by HPLC analysis and is reported in Fig. 2A PC-3 cells were exposed to 100 nM CN-CPT for 1, 3 and 6 hours. This dose was chosen since it resulted above the limit of instrumental detectability and in the linear range of a standard curve concomitantly run within the experiment. Results revealed that embedding CPT inside β-cyclodextrin nanosponges facilitated cellular uptake of the drug. Indeed the intracellular content of CPT increased in a time dependent manner until 6 hours from the treatment. This result confirmed that embedding CPT inside this nanoparticle system prevents the physiological degradation that may occur in the extracellular environment and facilitate the accumulation of the drug into the cells.

3.2 Topoisomerase I activity

Since CPT is a poorly stable molecule, we assessed whether chemical synthesis of CN-CPT altered its biological activity. Thus, DNA Topoisomerase I inhibitory activity was evaluated in PC-3 cells treated for 24 hours with 10 nM CPT or 10 nM CN-CPT (Fig. 2B). The enzymatic activity has been estimated with a semiquantitative method consisting in an electrophoretic run on agarose gel of supercoiled plasmids previously exposed to nuclear extracts. The Topoisomerase I activity relaxes the supercoiled plasmid resulting in a

different electrophoretic mobility, and this effect is lacking if the enzyme is inhibited. Results showed that CN-CPT, as CPT, retained the DNA Topoisomerase I inhibitory activity.

3.3 Evaluation of the phosphorylation status of the histone H2A.X

Since inhibition of Topoisomerase activity may induce DNA damage, this biological effect was analyzed in PC-3 and DU145 cells exposed to either CPT or CN-CPT for 24 and 48 hours. By Western blot evaluation of the phosphorylation status of the histone H2A.X on Ser 139 (a marker of DNA double strand breaks) 24 hours treatment with 1-10 nM CN-CPT induced a substantial induction of H2A.X phosphorylation in both PC-3 and DU145 cells whereas the same treatment with CPT was ineffective (Fig. 3A). The effect was even more pronounced after 48 hours. Confirmatory results were obtained by immunofluorescence experiments performed on PC-3 cells treated with 10 nM CPT or 10 nM CN-CPT for 24 hours that revealed nuclear localization of P-H2A.X in CN-CPT treated cells only (Fig. 3B).

3.4 Cytotoxicity of CPT and CN-CPT

The anti-tumor efficacy of CPT and CN-CPT on PC-3 and DU145 cells is reported in Fig. 4A. Results showed that both formulations were effective in reducing cell proliferation in a time- and dose-dependent manner. Following 96 hour treatment CPT decreased cell growth by 50% at 5 and 10 nM in PC-3 and DU145 respectively, and completely blocked cell growth starting from 20 nM in both cell models. CN-CPT showed a greater efficacy than CPT since it completely blocked proliferation already from the dose of 5 nM in both cell lines. The analysis of cell viability of PC-3 and DU145 cells treated with 1 and 20 nM CPT or 1 and 20 nM CN-CPT for 24 to 96 hours (Fig. 4B) showed that CN-CPT was

significantly more effective than CPT in both cell lines for both doses analyzed. Similar results were obtained with the analysis of cell clonogenicity (Fig. 4C) which revealed that CN-CPT completely blocked colony formation of both PC-3 and DU145 cells starting from 1 nM concentration whereas CPT was effective only starting from 20 nM.

3.5 Effect of CPT and CN-CPT on cell cycle and cell death

Several reports showed that CPT exerts anti-tumor effects by inducing cell cycle arrest. In order to compare the efficacy of CN-CPT with CPT, cell cycle analysis was performed (Fig. 5). Results showed that treatment with 10 nM CN-CPT for 24 hours caused a significant accumulation of both PC-3 and DU145 cells in the S-phase of the cell cycle. In contrast, treatment with the same concentration of CPT caused accumulation of cells in G2/M phase. These data are consistent with previous reports where partial inhibition of Topoisomerase activity has been shown similar to cell cycle arrest (Hayashi et al., 2002). Furthermore, CN-CPT caused cell cycle arrest even at 1nM concentration, which was not effective for CPT. In particular, the treatment for 24 hours with 1 nM CN-CPT showed an increased proportion of cells in S and G2/M phases for PC-3 and DU145 cells, respectively.

Then, we assessed whether CPT also induced cell death. PC-3 and DU145 cells treated with either CPT or CN-CPT for 96 hours and cell death was evaluated by Annexin V/Propidium Iodide staining every 24 hours. As shown in Fig. 6 CN-CPT ability to induce cell death was higher than CPT in both PC-3 and DU145 cells. Treatment with 10 nM CN-CPT caused 70 and 80% cell death at 96 hours in PC-3 and DU145 cells, respectively, whereas cell death caused by CPT was 15% and 30%, respectively. Moreover, 1nM CN-

CPT was already effective since it caused 60 and 75% cell death in PC-3 and DU145 cells respectively, whereas this dose was ineffective for CPT.

3.6 CPT and CN-CPT effects on LNCaP cells

DU145 and PC-3 cells do not express Androgen Receptor (AR) and represent a models of androgen refractory PCa. Since AR expression is a crucial parameter in PCa progression and therapeutic intervention, we compared CTP and CN-CPT effectiveness also in the AR-expressing cell line LNCaP. The effects on cell proliferation, viability and clonogenicity are showed in Fig. 7A, 7B and 7C respectively. Results showed that LNCaP are less susceptible to the anti-tumour activity of CPT than PC3 and DU145, since CPT inhibited LNCaP cells proliferation starting from 150 nM concentration and their clonogenicity starting at 75 nM. In contrast, CN-CPT inhibited proliferation starting from the 5nM dose and blocked growth and clonogenicity starting from the 10 nM dose. LNCaP cells viability after treatment with 10, 75 and 150 nM CPT or 10, 75 and 150 nM CN-CPT for 24 to 96 hours showed that CN-CPT was significantly more effective than CPT for all doses analyzed.

Finally, LNCaP cells exposed to CPT or CN-CPT were analyzed for phosphorylation of histone H2A.X (ser139) and AR expression. Results (Fig. 8) showed that 10 nM CPT was unable to induce phosphorylation of H2A.X whereas CN-CPT induced a robust dose-dependent phosphorylation of H2A.X at the 1 nM dose. Moreover, CN-CPT caused also a significant repression of AR expression that was evident starting from the dose of 1nM, whereas CPT was ineffective even at the 10 nM dose.

4. Discussion

Camptothecin is a Topoisomerase I inhibitor with potent antitumor activity that has raised great interest in the past two decades for the treatment of solid and hematological malignancies. However, this drug did not reach routine clinical use because of toxicity and an unsatisfactory pharmacological profile. In recent years, several camptothecin analogues have been developed but only two drugs, topotecan and irinotecan, have reached clinical approval (Venditto and Simanek, 2010). These compounds, although showing a better pharmacological profile and a greater efficacy compared to camptothecin, either require continuous infusion or frequent administrations to reach effective concentrations (Brandi et al., 2011; Burris et al., 1994; Kummar et al., 2011; Pitot et al., 2000). Since the main limitation in the use of CPT and CPT analogues is due to their chemical instability, we hypothesized that β-cyclodextrin nanosponge-delivery may represent a valuable approach to overcome CPT instability. Our results suggest that β-cyclodextrin nanosponge effectively strengthens the anti-tumor efficacy of camptothecin.

We initially used the androgen-independent prostate cancer cell lines PC-3 and DU145, which are poorly differentiated cells derived from metastatic lesions and are representative of advanced disease. HPLC data, performed on PC-3 cells, demonstrated that the intracellular content of CPT increases over a 6-hour time frame. Moreover, experiments evaluating CPT Topoisomerase I inhibition activity showed that CN-CPT fully maintained this activity. These data suggests that β-cyclodextrin nanosponge not only protects the drug when internalized but allows its release for a prolonged time frame leading to a longer exposure to CPT. Similar results were reported in previous findings where cyclodextrin carriers mediated a prolonged exposure of cancer cells to the chemotherapy drug

paclitaxel (Torne et al., 2010) and docetaxel (Huang et al., 2011). Additionally, Torne *et al* demonstrated that β-cyclodextrin nanosponge technology increased the plasma concentration of paclitaxel and improved its oral bioavailability (Torne et al., 2010).

Cell proliferation and clonogenic assays revealed that PC-3 cells displayed higher sensitivity to free camptothecin than DU145 cells. Inhibition of cell growth and colony formation was observed starting from the 10 and 20 nM doses respectively. However, both models showed a greater responsiveness to β-cyclodextrin-carried camptothecin, which blocked colony formation and cell growth starting at the 1 nM dose. Importantly, treatment with drug-free β-cyclodextrin nanosponge showed no signs of toxicity in both cell lines, confirming that the effects displayed by CN-CPT are drug specific. Indeed, the β-cyclodextrin toxicology profile has been characterized in several *in vitro* and *in vivo* reports and always resulted to be nontoxic and well tolerated even at very high doses (Park et al., 2011).

The inhibition of Topoisomese I activity exerted by CPT may result in DNA damage and cell cycle arrest followed by cell death, but high doses are required to exert these effects (Legarza and Yang, 2006). In our experiments, we observed that β-cyclodextrin nanosponge-protected CPT induced sustained DNA damage, cell cycle arrest, and cell death even at doses around 10 nM. These strengthened effects confirm the efficacy of the β-cyclodextrin nanosponge-based technology to protect camptothecin and show that the drug may be effective at doses likely to be easily reached *in vivo.*

Androgen receptor activity is critical in the progression of PCa. For decades androgen deprivation therapy has been the primary treatment for men with metastatic prostate

cancer (Nguyen and Wang, 2008). Although advanced disease is initially sensitive to androgen deprivation therapy, most deaths occur following progression toward castration-resistant metastatic prostate cancer, which is currently incurable (Massard and Fizazi, 2011).

Based on previous reports showing that camptothecin disrupts androgen receptor signaling (Liu et al., 2010), we evaluated the ability of CPT and CN-CPT in modulating AR expression in LNCaP cells. Our data revealed that LNCaP cells displayed minimal susceptibility to CPT, whereas CN-CPT showed a substantial anti-tumor activity even in these cells. Moreover, CN-CPT inhibited AR expression at 10 nM, whereas CPT was inactive at these doses. These data do not contradict data from other authors detecting inhibition of AR expression using micromolar concentrations of CPT (Liu et al., 2010).

Recent evidences suggest that the AR signaling system remains intact and activated despite low levels of androgens in castrate-resistant prostate cancer (Kageyama et al., 2007). Currently, modifications to the AR via mutations, amplification and phosphorylation have been proposed as underlying mechanisms of hormone-resistance of prostate cancer cells (Massard and Fizazi, 2011; Nguyen and Wang, 2008; Sharifi, 2010). Thus the development of novel or more effective treatment modalities targeting the AR and AR-related molecules may provide better management of androgen-independent prostate cancer. The effect of CN-CPT on AR is intriguing and may contribute to its potential antitumor activity in prostate cancer.

In conclusion, this study suggests that β-cyclodextrin nanosponge represents a promising model for camptothecin delivery and provides evidences to initiate further investigation to evaluate its *in vivo* efficacy in preclinical models of prostate cancer. Nanoparticles based

on cyclodextrin technology can also be conjugated with ligands allowing their specific targeting to cancer cells. Davis reported use of transferrin-conjugated β-cyclodextrin that was able to bind the transferrin receptor on cancer cells facilitating internalization of the nanoparticles by endocytosis (Davis, 2009). CN-CPT effectiveness against prostate tumors might be further increased by conjugation with ligands targeting prostate tumor cells, such as androgen receptor ligands that have been found on prostate cancer cell membranes. A novel membrane-associated Androgen Receptor that is frequently found up-regulated in castration-resistant prostate cancer cells (Yang et al., 2011). This formulation can improve the specificity of prostate cancer and consequently further reduce the toxicity and improve the efficacy of CPT.

Conflict of interest

The authors declare no conflict of interest.

Acknowledgements

This research was in part supported by a generous gift from the Liodakis family.

References

Bharali, D.J., Khalil, M., Gurbuz, M., Simone, T.M., Mousa, S.A., 2009. Nanoparticles and cancer therapy: a concise review with emphasis on dendrimers. Int J Nanomedicine. 4, 1-7.

Brandi, G., Biasco, G., Mirarchi, M.G., Golfieri, R., Di Paolo, A., Borghi, A., Fanello, S., Derenzini, E., Agostini, V., Giampalma, E., Cappelli, A., Pini, P., Costantini, S., Danesi, R., Bolondi, L., Piscaglia, F., 2011. A phase I study of continuous hepatic arterial infusion of Irinotecan in patients with locally advanced hepatocellular carcinoma. Dig Liver Dis. 43, 1015-1021.

Burris, H.A. 3rd., Awada, A., Kuhn, J.G., Eckardt, J.R., Cobb, P.W., Rinaldi, D.A., Fields, S., Smith, L., Von Hoff, D.D., 1994. Phase I and pharmacokinetic studies of topotecan administered as a 72 or 120 h continuous infusion. Anticancer Drugs. 5, 394-402.

Cavalli, R., Trotta, F., Tumiatti, W., 2006. Cyclodextrin-based Nanosponges for Drug Delivery. J. Incl. Phenom. Macrocycl. Chem. 56, 209–213.

Davis, M.E., 2009. The first targeted delivery of siRNA in humans via a self-assembling, cyclodextrin polymer-based nanoparticle: from concept to clinic. Mol Pharm. 6, 659-668.

Droz, J.P., Chaladaj, A., 2008. Management of metastatic prostate cancer: the crucial role of geriatric assessment. BJU Int. 101 Suppl 2, 23-29.

Feldman, B.J., Feldman, D., 2001. The development of androgen-independent prostate cancer. Nat Rev Cancer. 1, 34-45.

Hayashi, K., Kuniyasu, H., Oue, N., Shigeishi, H., Kuraoka, K., Nakayama, H., Yasui, W., 2002. Induction of hRAD9 is required for G2/M checkpoint signal transduction in gastric cancer cells. Pathobiology. 70, 40-46.

Hertzberg, R.P., Caranfa, M.J., Hecht, S.M., 1989. On the mechanism of topoisomerase I inhibition by camptothecin: evidence for binding to an enzyme-DNA complex. Biochemistry. 28, 4629-4638.

Huang, X.X., Zhou, C.L., Wang, H., Chen, C., Yu, S.Q., Xu, Q., Zhu, Y.Y., Ren, Y., 2011. Pharmacokinetics, efficacy, and safety evaluation of docetaxel/hydroxypropyl-sulfobutyl-β-cyclodextrin inclusion complex. AAPS PharmSciTech. 12, 665-672.

Jones, C.B., Clements, M.K., Wasi, S., Daoud, S.S., 2000. Enhancement of camptothecin-induced cytotoxicity with UCN-01 in breast cancer cells: abrogation of S/G(2) arrest. Cancer Chemother Pharmacol. 45, 252-258.

Kageyama, Y., Hyochi, N., Kihara, K., Sugiyama, H., 2007. The androgen receptor as putative therapeutic target in hormone-refractory prostate cancer. Recent Pat Anticancer Drug Discov. 2, 203-211.

Koo, O.M., Rubinstein, I., Onyuksel, H., 2005. Camptothecin in sterically stabilized phospholipid micelles: a novel nanomedicine. Nanomedicine. 1, 77-84.

Kummar, S., Raffeld, M., Juwara, L., Horneffer, Y., Strassberger, A., Allen, D., Steinberg, S.M., Rapisarda, A., Spencer, S.D., Figg, W.D., Chen, X., Turkbey, I.B., Choyke, P., Murgo, A.J., Doroshow, J.H., Melillo, G., 2011. Multihistology, target-driven pilot trial of oral topotecan as an inhibitor of hypoxia-inducible factor-1α in advanced solid tumors. Clin Cancer Res. 17, 5123-513.

Legarza, K., Yang, L.X., 2006. New molecular mechanisms of action of camptothecin-type drugs. Anticancer Res. 26, 3301-3305.

Liu, S., Yuan, Y., Okumura, Y., Shinkai, N., Yamauchi, H., 2010. Camptothecin disrupts androgen receptor signaling and suppresses prostate cancer cell growth. Biochem Biophys Res Commun. 394, 297-302.

Massard, C., Fizazi, K., 2011. Targeting continued androgen receptor signaling in prostate cancer. Clin Cancer Res. 17, 3876-3883.

Nguyen, M.M., Wang, Z., 2008. Manipulation of androgens and alterations in the androgen receptor axis in prostate cancer. Minerva Urol Nefrol. 60, 15-29.

Park, J.H., Choi, K.H., Kwak, H.S., 2011. Single- and 14-Day Repeat-Dose Toxicity of Cross-Linked β-Cyclodextrin in Rats. Int J Toxicol. 30, 700-706.

Pitot, H.C., Goldberg, R.M., Reid, J.M., Sloan, J.A., Skaff, P.A., Erlichman, C., Rubin, J., Burch, P.A., Adjei, A.A., Alberts, S.A., Schaaf, L.J., Elfring, G., Miller, L.L., 2000. Phase I dose-finding and pharmacokinetic trial of irinotecan hydrochloride (CPT-11) using a once-every-three-week dosing schedule for patients with advanced solid tumor malignancy. Clin Cancer Res. 6, 2236-2244.

Pommier, Y., 2006. Topoisomerase I inhibitors: camptothecins and beyond. Nat Rev Cancer. 6, 789-802.

Sharifi, N., 2010. New agents and strategies for the hormonal treatment of castration-resistant prostate cancer. Expert Opin Investig Drugs. 19, 837-846.

Shen, M.M., Abate-Shen, C., 2010. Molecular genetics of prostate cancer: new prospects for old challenges. Genes Dev. 24, 1967-2000.

Swaminathan, S., Vavia, P.R., Trotta, F., Torne, S., 2007. Formulation of betacyclodextrin based nanosponges of itraconazole. J. Incl. Phenom. Macrocycl. Chem. 57, 89–94.

Swaminathan, S., Pastero, L., Serpe, L., Trotta, F., Vavia, P., Aquilano, D., Trotta, M., Zara, G., Cavalli, R., 2010. Cyclodextrin-based nanosponges encapsulating camptothecin: physicochemical characterization, stability and cytotoxicity. Eur J Pharm Biopharm. 74, 193-201.

Takahashi, P., Polson, A., Reisman, D., 2011. Elevated transcription of the p53 gene in early S-phase leads to a rapid DNA-damage response during S-phase of the cell cycle. Apoptosis. 16, 950-958.

Taplin, M.E., 2007. Drug insight: role of the androgen receptor in the development and progression of prostate cancer. Nat Clin Pract Oncol. 4, 236-244.

Torne, S.J., Ansari, K.A., Vavia, P.R., Trotta, F., Cavalli, R., 2010. Enhanced oral paclitaxel bioavailability after administration of paclitaxel-loaded nanosponges. Drug Deliv. 17, 419-425.

Trotta, F., Cavalli, R., 2009. Characterization and Applications of New Hyper-Cross-Linked Cyclodextrins. Compos. Interfaces. 16, 39–48.

Venditto, V.J., Simanek, E.E., 2010. Cancer Therapies Utilizing the Camptothecins: A Review of the in Vivo Literature. Mol Pharm. 7, 307-349.

Wall, M.E., Wani, M.C., Cook, C.E., Palmer, K.H., McPhail, A.T., Sim, G.A., 1966. Plant antitumor agents. I. The isolation and structure of camptothecin, a novel alkaloidal leukemia and tumor inhibitor from Camptotheca accuminata. J. Am. Chem. Soc. 88, 3888–3890.

Yang, X., Guo, Z., Sun, F., Li, W., Alfano, A., Shimelis, H., Chen, M., Brodie, A.M., Chen, H., Xiao, Z., Veenstra, T.D., Qiu, Y., 2011. Novel membrane-associated androgen receptor splice variant potentiates proliferative and survival responses in prostate cancer cells. J Biol Chem. 286, 36152-36160.

Zhang, L., Gu, F.X., Chan, J.M., Wang, A.Z., Langer, R.S., Farokhzad, O.C., 2008. Nanoparticles in medicine: therapeutic applications and developments. Clin Pharmacol Ther. 83, 761-769.

Zhou, Y., Gwadry, F.G., Reinhold, W.C., Miller, L.D., Smith, L.H., Scherf, U., Liu, E.T., Kohn, K.W., Pommier, Y., Weinstein, J.N., 2002. Transcriptional regulation of mitotic

genes by camptothecin-induced DNA damage: microarray analysis of dose- and time-dependent effects. Cancer Res. 62, 1688-1695.

Legends

Fig. 1. Aspect of camptothecin loaded β-cyclodextrin nanosponge. **A:** Camptothecin loaded β-cyclodextrin nanosponge (CN-CPT) was a stable aqueous nanosuspension with low polydispersity index. **B:** Transmission electron microscopy (TEM) analysis of CN-CPT showed a spherical morphology and confirmed the small size.

Fig. 2. CPT intracellular uptake and Topoisomerase I activity. **A**: HPLC detection of camptothecin after treatment with 100 nM of CN-CPT for 1, 3 and 6 hours in PC-3 cells. **B**: Inhibition of Topoisomerase I activity in PC-3 cells treated for 24 hours with 10 nM CPT and CN-CPT.

Fig. 3. Induction of DNA damage following CPT and CN-CPT treatment**. A:** Representative Western blot analysis of phospho-H2A.X (ser139) of PC-3 and DU145 cell lines untreated or treated with either 10 nM CPT or 1 and 10 nM CN-CPT for 24 and 48 hours. The same blots were probed with anti β-actin antibody as a loading control. **B:** Fluorescence microscopy image of PC-3 cells untreated and treated with 10 nM CPT or CN-CPT for 24 hours and stained with phospho-H2A.X (ser139) (red) and 4',6'-diamidino-2-phenylindole (DAPI; shown in blue), as nuclear staining, showing the induction of DNA damage.

Fig. 4. Inhibition of proliferation and clonogenicity following CPT and CN-CPT treatment. **A**: Effect of CPT and CN-CPT on PC-3 and DU145 cell lines proliferation was tested by MTT assay. Cells (800/well) were treated with increasing concentrations of CPT and CN-CPT for 24-96 hours and the result was expressed as absorbance at 570 nm. Values are

expressed as mean ± SD; each group n = 8, experiments in triplicate. **B:** Effect of CPT and CN-CPT on PC-3 and DU145 cell lines viability. Data were expressed as the percentage of cells viability versus control. One-way ANOVA and the Dunnett's test revealed statistically significance differences (* $p<0.05$; ** $p<0.01$) of CN-CPT versus CPT treated cells. **C**: Effect of CPT and CN-CPT on prostate cancer cells clonogenicity was tested by colony forming assay. DU145 and PC-3 cells (500/well) were seeded in 6 well plates and treated with both compounds at the indicated concentrations for 72 hours. Cells were cultured for 10 days and subsequently fixed and stained with crystal violet.

Fig. 5. *Induction of S phase cell cycle arrest by CPT and CN-CPT*. **A-B:** Representative cell cycle plots of PC-3 and DU145 cell lines untreated or treated with 10 nM CPT or CN-CPT for 24 hours. **C-D:** Quantification of cell cycle phases of PC-3 and DU145 cells untreated or treated with 1 and 10 nM CPT or CN-CPT for 24 hours.

Fig. 6. *Induction of cell death following treatment with CPT and CN-CPT*. **A-C:** Representative Annexin V/Propidium Iodide plots of DU145 and PC-3 cells either untreated or treated with 10 nM CPT or CN-CPT for 96 hours. **B-D:** Cell death quantification of DU145 and PC-3 cells following 24-96 hours treatment with both compounds at 1 and 10 nM concentrations.

Fig. 7. *Inhibition of LNCaP proliferation and clonogenicity following CPT and CN-CPT treatment*. **A**: Effect of CPT and CN-CPT on LNCaP cell proliferation was tested by MTT assay. Cells (800/well) were treated with either CPT and CN-CPT for 24-96 hours at the indicated concentrations and the result was expressed as absorbance at 570 nm. Values are expressed as mean ± SD; each group n = 8, experiments in triplicate. **B:** Effect of CPT

and CN-CPT on LNCaP cells viability. Data were expressed as the percentage of cells viability versus control. One-way ANOVA and the Dunnett's test revealed statistically significance differences (* $p<0.05$; ** $p<0.01$) of CN-CPT versus CPT treated cells. **C**: Effect of CPT and CN-CPT on LNCaP cell clonogenicity was tested by colony forming assay. 500 cell/well were seeded in 6 well plates and treated with both compounds at the indicated concentrations for 72 hours. Cells were cultured for 10 days and subsequently fixed and stained with crystal violet.

Fig. 8. *Induction of DNA damage and inhibition of androgen receptor expression in LNCaP cells.* Representative Western blot analysis of phospho-H2A.X (ser139) and AR expression of LNCaP cell untreated or treated with either 10 nM CPT or 1 and 10 nM CN-CPT for 24 and 48 hours. The same blots were probed with anti β-actin antibody as a loading control.

Figure(s)
Click here to download high resolution image

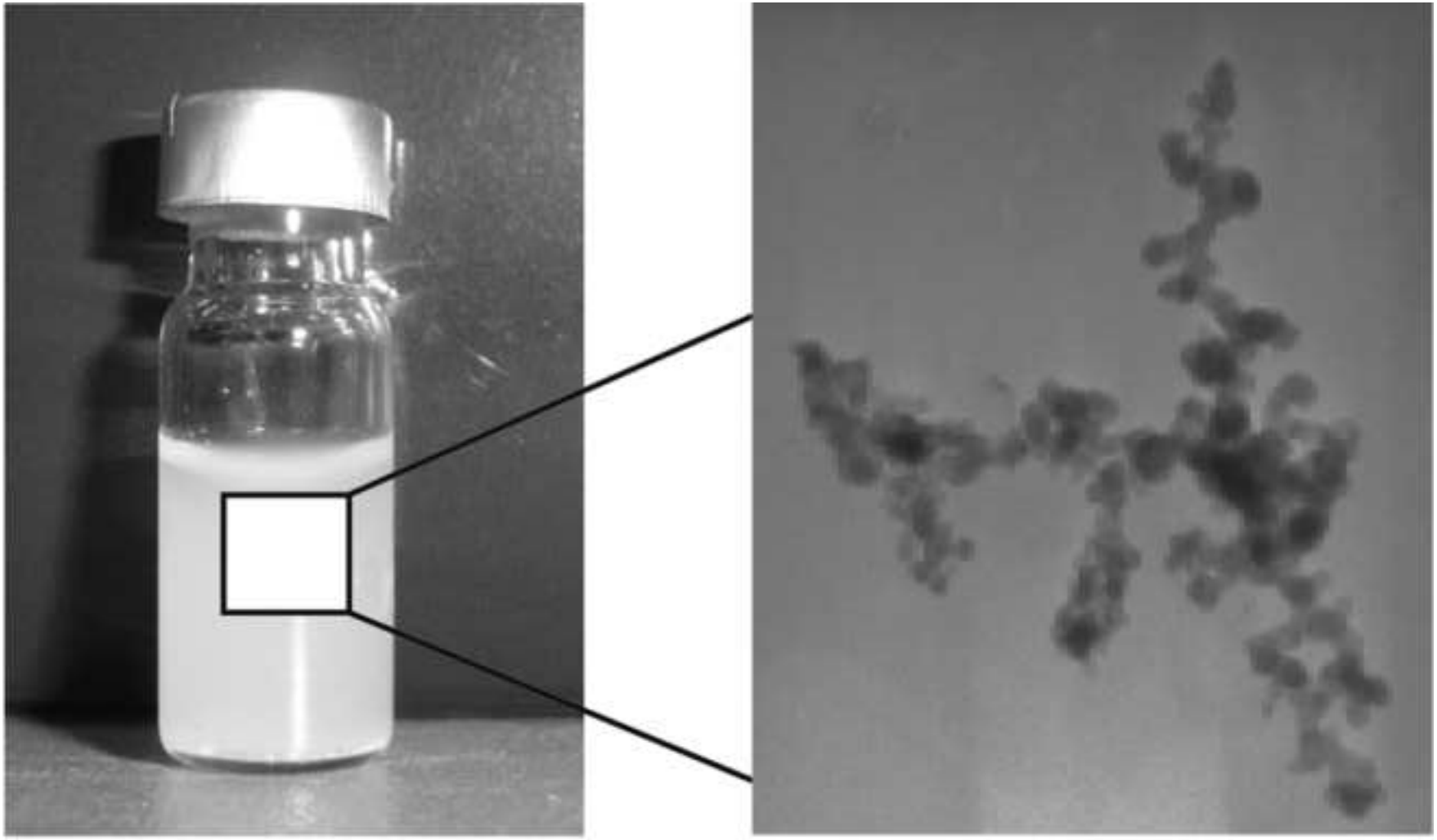

Figure 1

Figure(s)
Click here to download high resolution image

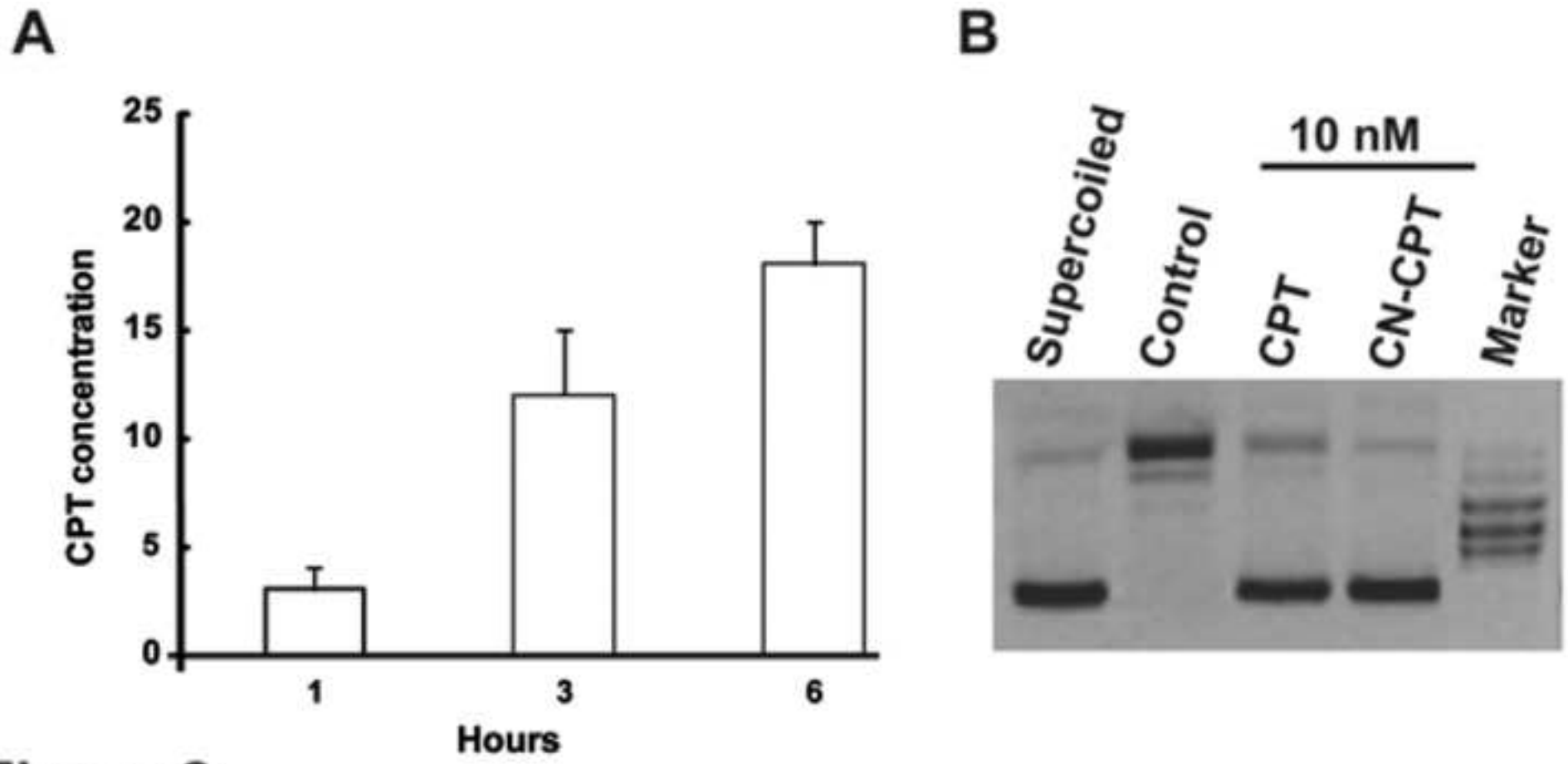

Figure 2

Figure(s)

Click here to download high resolution image

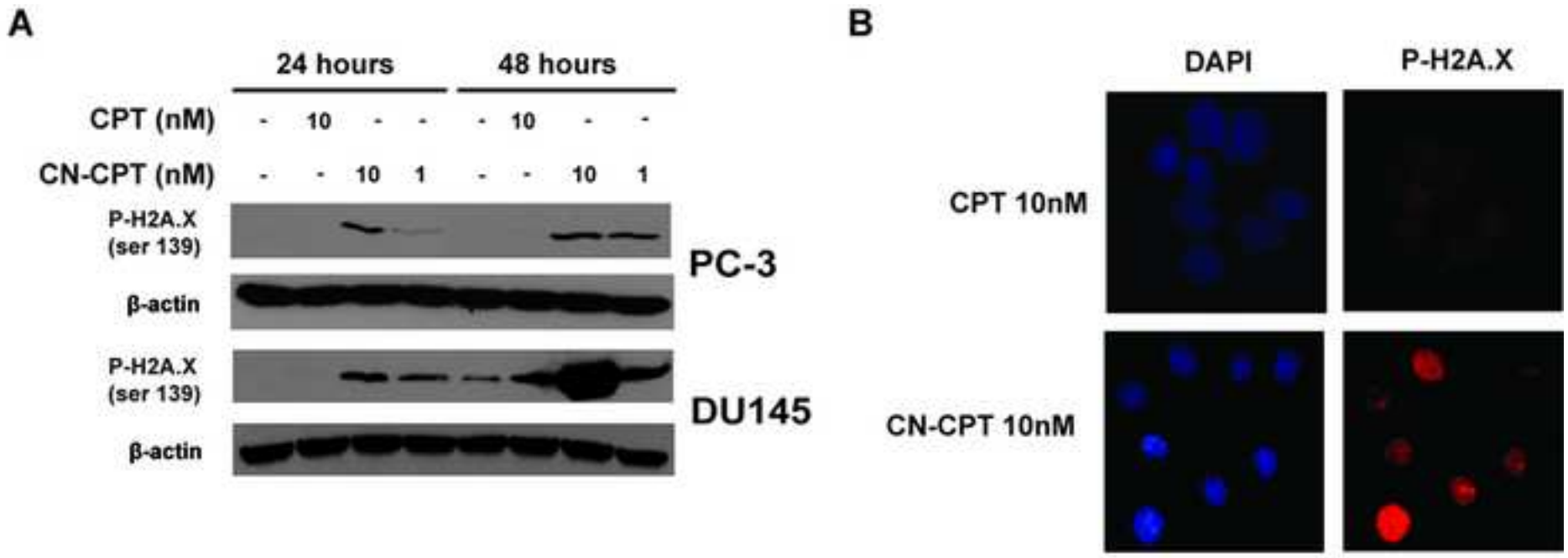

Figure 3

Figure(s)

Click here to download high resolution image

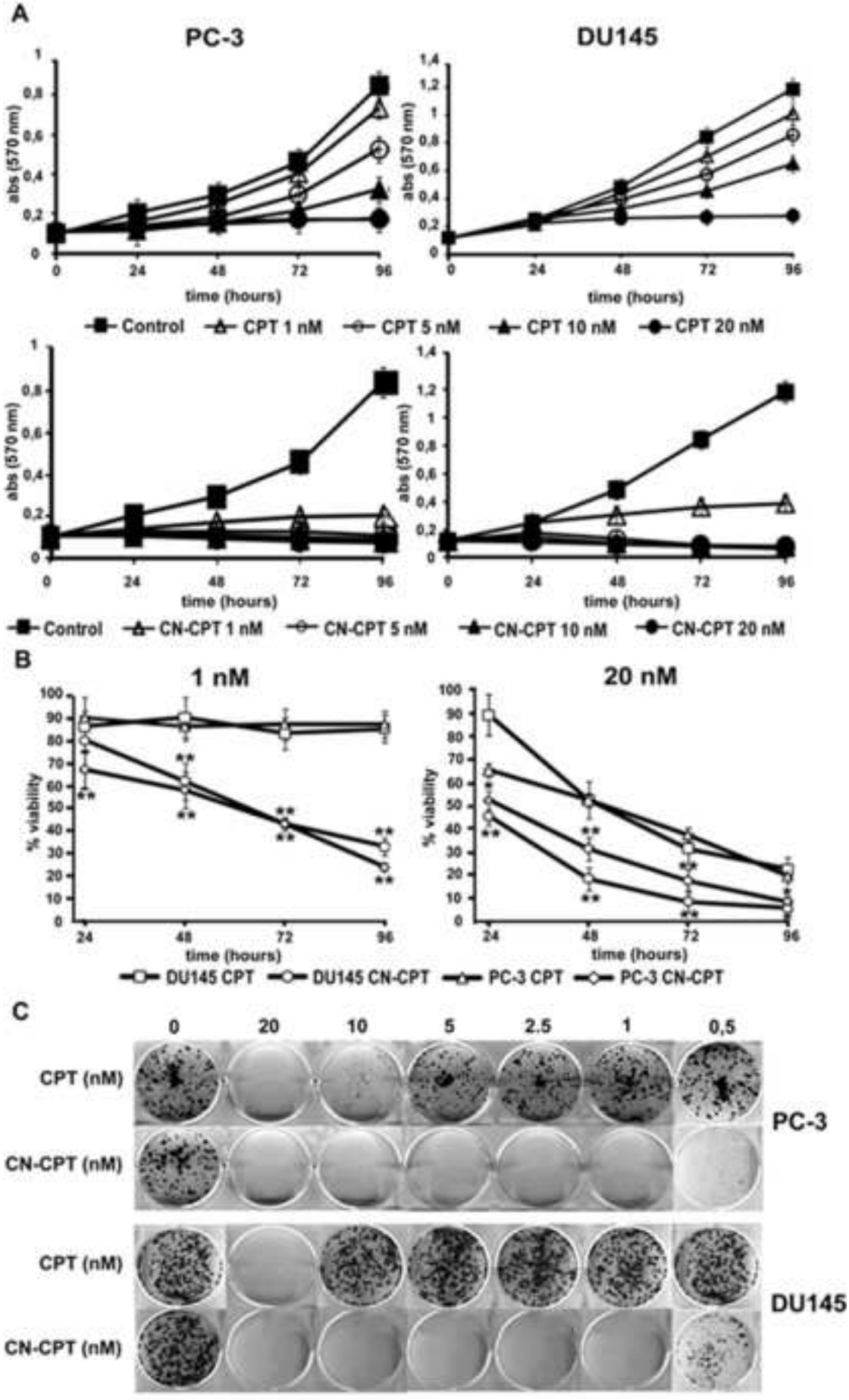

Figure 4

Figure(s)

Click here to download high resolution image

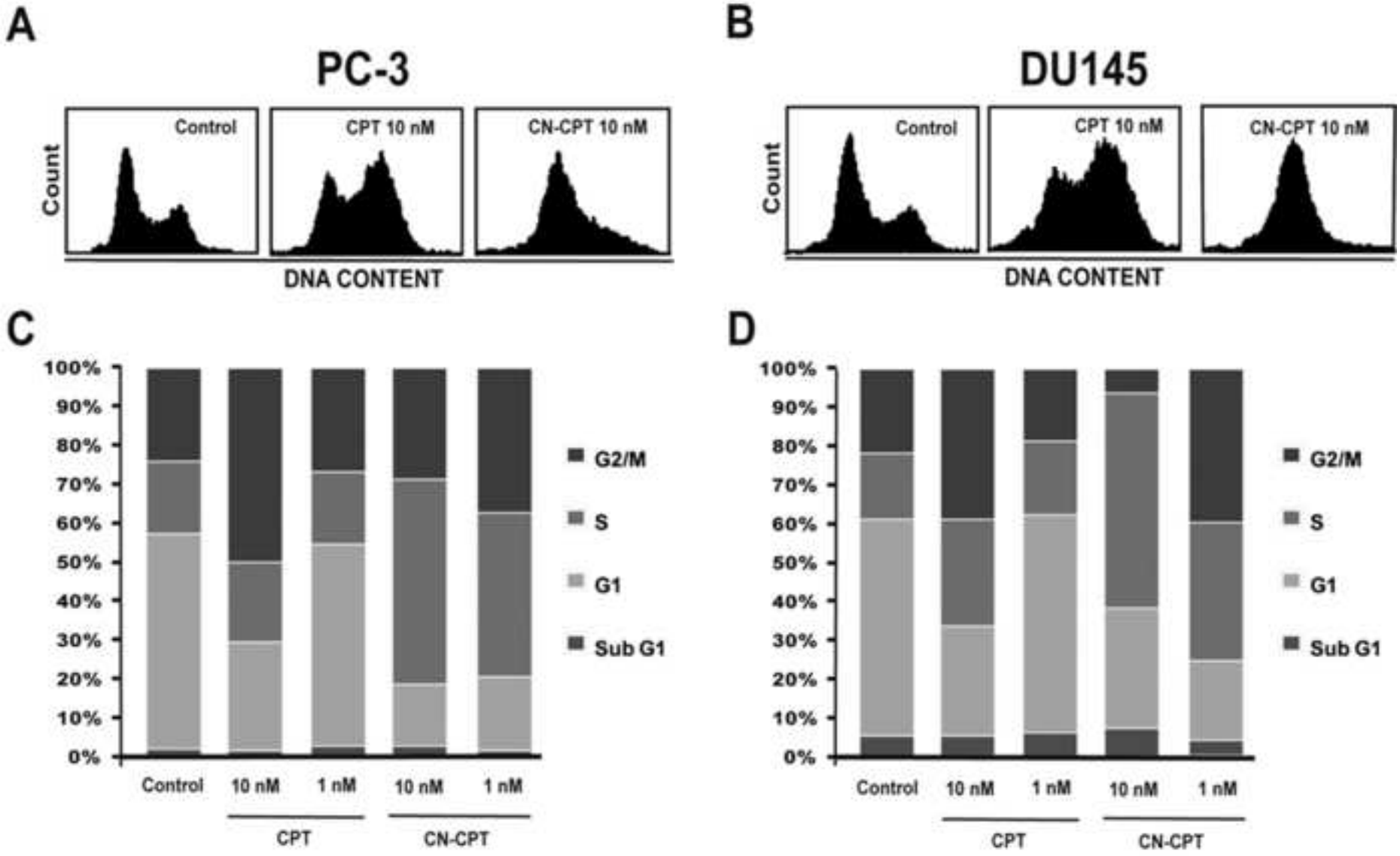

Figure 5

Figure(s)

Click here to download high resolution image

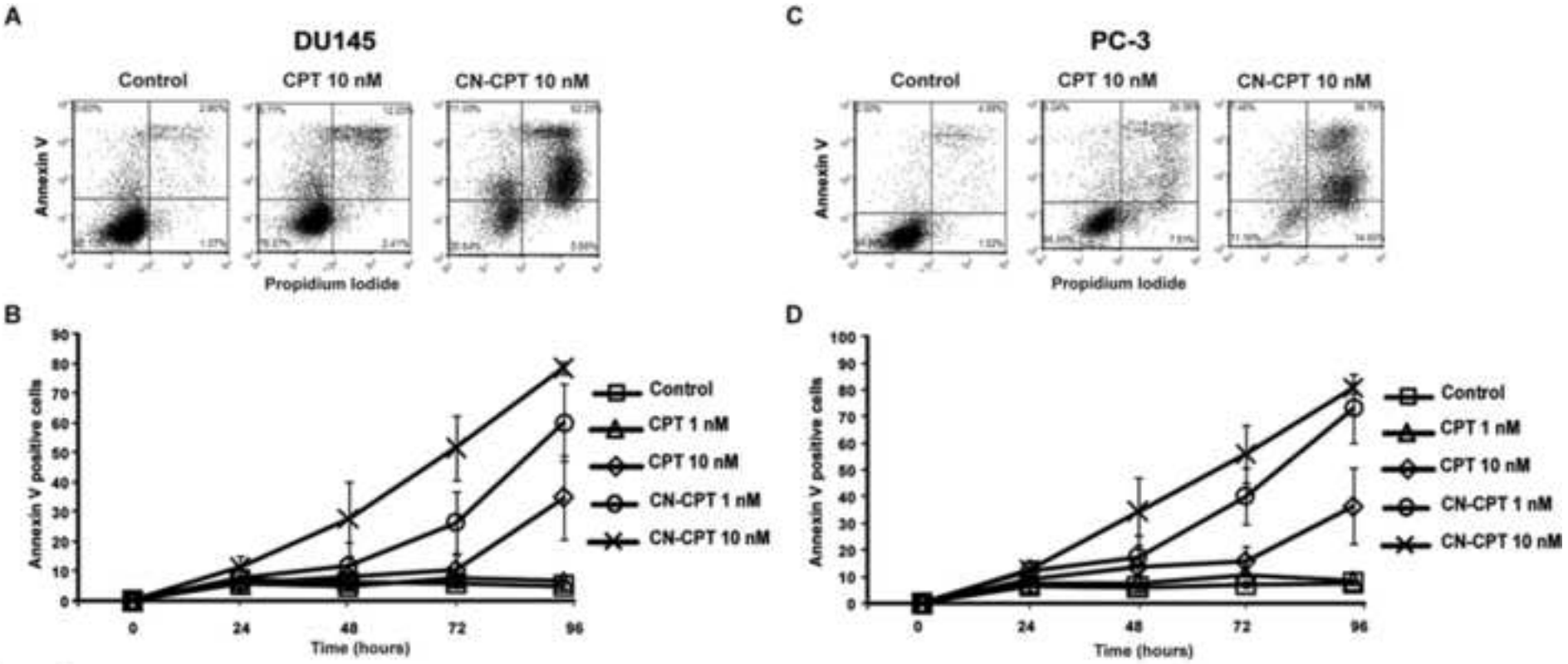

Figure 6

Figure(s)

Click here to download high resolution image

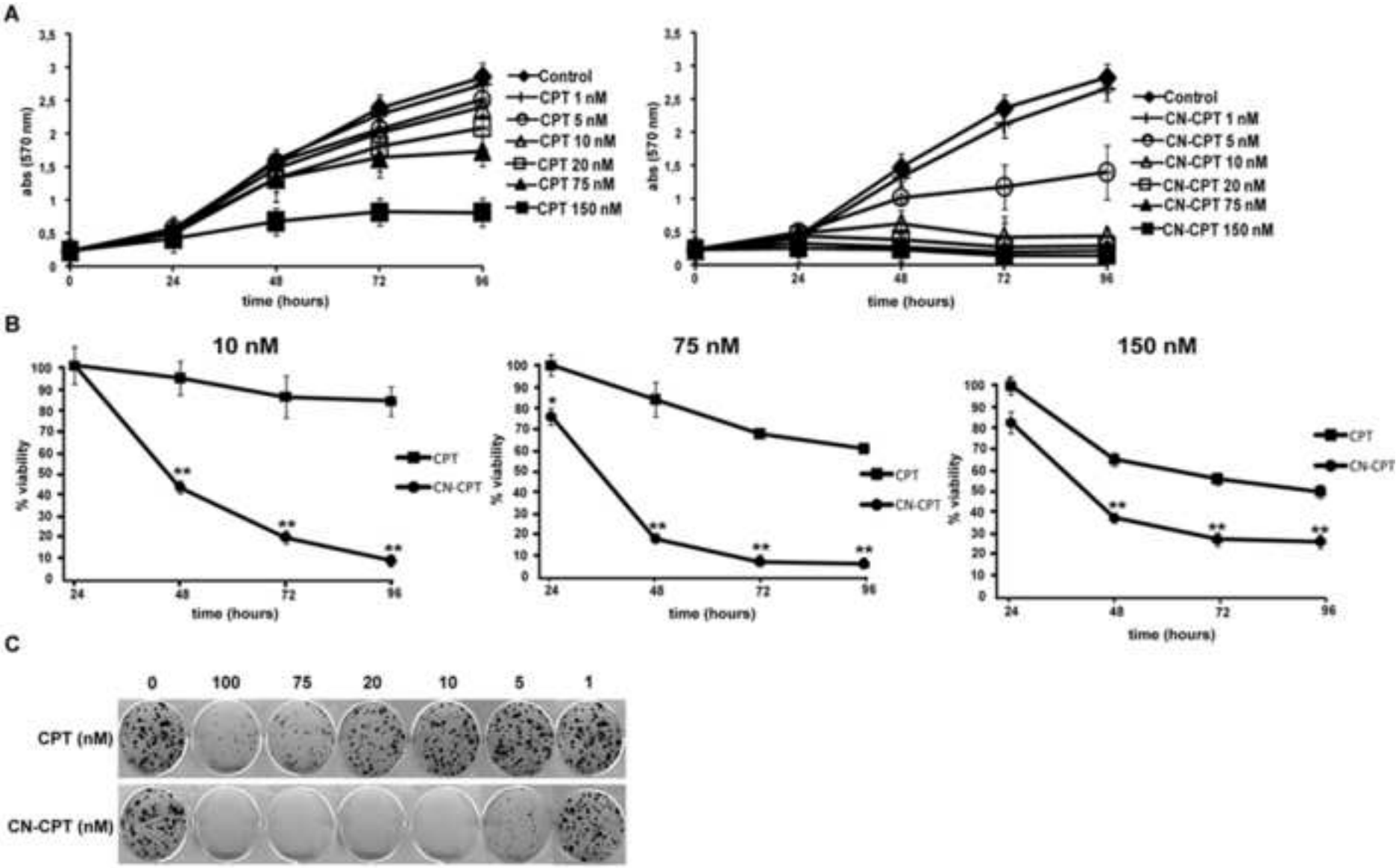

Figure 7

Figure(s)

Click here to download high resolution image

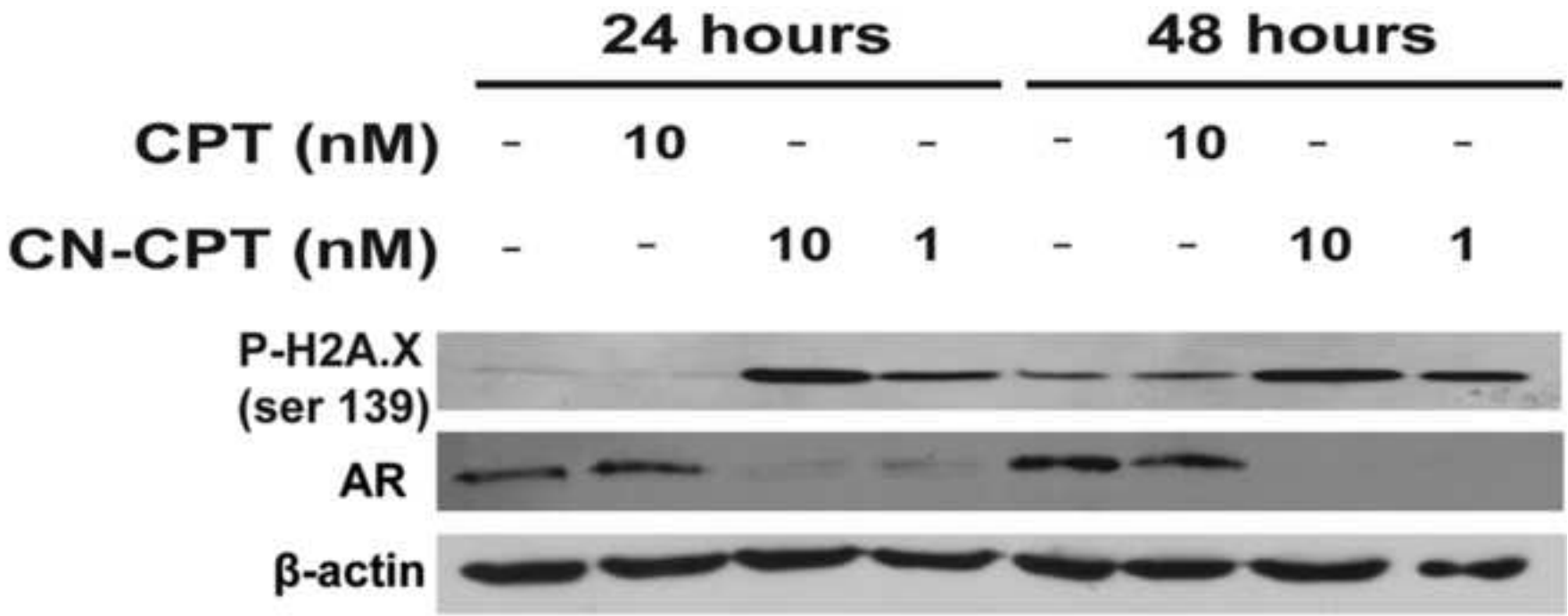

Figure 8